

Tensor-force effects in the ${}^2\text{H}(\vec{d}, \gamma){}^4\text{He}$ reaction and the D state of ${}^4\text{He}$

S. Mellema,* T. R. Wang, and W. Haeberli

Department of Physics, University of Wisconsin—Madison, Madison, Wisconsin 53706

(Received 27 June 1986)

Vector analyzing powers, tensor analyzing powers, and relative differential cross sections have been measured for the ${}^2\text{H}(\vec{d}, \gamma){}^4\text{He}$ reaction at an incident energy of 10 MeV. Multipole decomposition and partial-wave analysis reveal that about 15% of the cross section involves processes in which the tensor force plays a role, either in the entrance or exit channel. Contrary to earlier claims, the reaction cannot be used to determine the D -state admixture in the ${}^4\text{He}$ wave function unless the D state of the deuteron and other tensor-force effects in the entrance channel are taken into account.

I. INTRODUCTION

The first measurement of the tensor analyzing power T_{20} for the ${}^2\text{H}(\vec{d}, \gamma){}^4\text{He}$ reaction, made at 9.7 MeV by Weller *et al.*,¹ has stimulated interest in this reaction as a tool to study the D state of ${}^4\text{He}$. Indeed, although the ground state of ${}^4\text{He}$ is predominantly 1S_0 (where the notation used is ${}^{2S+1}L_J$), the inclusion of the tensor component of the nucleon-nucleon interaction generates a 3D_0 component in this state.² Weller *et al.*¹ analyze their data under a number of simplifying assumptions and conclude that about 3% of the total cross section arises from capture to this D state.

The analysis of Weller *et al.*,¹ as well as the recent calculations of Santos *et al.*,² assume that the transition is restricted to pure $E2$ radiation. In a recent Letter³ we have shown that this assumption is not valid, and have expressed concern regarding its use in drawing conclusions about D -state effects. Furthermore, the analyses of Refs. 1 and 2 have neglected tensor-force effects in the incident channel. The tensor component of the nucleon-nucleon force also gives rise to a D state in the deuteron ground state and to mixing between angular momentum states of the d-d system.

Because of the identity of the incident and target particles, a measurement of angular distributions of the differential cross section and vector and tensor analyzing powers for this reaction leads to a complete determination of the transition matrix, without resorting to any simplifying assumptions other than the restriction of both electric and magnetic transitions to multipolarity $L \leq 2$. This in turn leads to an estimate of the magnitude of the tensor-force effects in the reaction. Because of the fact that these effects occur in both the entrance and exit channels, however, it is not possible to make any direct conclusion (in a model-independent way) regarding capture to the ${}^4\text{He}$ D state.

II. EXPERIMENTAL TECHNIQUES

The measurements made use of a 10 MeV polarized deuteron beam from the University of Wisconsin EN tandem accelerator and crossed-beam polarized ion source.⁴

The target was a gas cell of diameter 3.7 cm with 3 μm tungsten entrance and exit foils, filled with 200 kPa of D_2 at liquid-nitrogen temperature. The outgoing γ rays were detected using a 25 \times 25 cm NaI detector surrounded by a plastic anticoincidence shield.⁵ The spectrometer also incorporated neutron shielding in the form of ${}^6\text{Li}_2\text{CO}_3$ as well as a lead shield and collimator, and subtended a solid angle of 31.1 msr. In addition, 42 cm of paraffin shielding was placed between the target and detector in order to reduce the flux of ${}^2\text{H}(d, n){}^3\text{He}$ neutrons into the detector. The detector electronics involved both anticoincidence with the plastic shield and pileup rejection similar to that of Ref. 6. The detector/shielding assembly could be rotated in an angular range from 25° to 155°, and measurements were taken at 11 angles in this range.

The differential cross section for a reaction involving incident polarized spin-1 particles may be written as:

$$\sigma(\theta) = \sigma_u(\theta) [1 + 2iT_{11}(\theta)\text{Re}(it_{11}) + T_{20}(\theta)t_{20} + 2T_{21}(\theta)\text{Re}(t_{21}) + 2T_{22}(\theta)\text{Re}(t_{22})], \quad (1)$$

where $\sigma_u(\theta)$ is the unpolarized cross section, the T_{kq} are the analyzing powers of the reaction, and the t_{kq} describe the beam polarization. If one assumes that the polarization of the deuteron beam possesses an axis of symmetry, the beam moments may be written as:

$$\begin{aligned} \text{Re}(it_{11}) &= \frac{1}{\sqrt{2}}\tau_{10}\sin\beta\cos\phi, \\ t_{20} &= \frac{1}{2}\tau_{20}(3\cos^2\beta - 1), \\ \text{Re}(t_{21}) &= \left(\frac{3}{2}\right)^{1/2}\tau_{20}\sin\beta\cos\beta\sin\phi, \\ \text{Re}(t_{22}) &= -\left(\frac{3}{8}\right)^{1/2}\tau_{20}\sin^2\beta\cos 2\phi, \end{aligned} \quad (2)$$

where τ_{10} and τ_{20} are the vector and tensor polarizations with respect to the spin-symmetry axis at the ion source, β is the angle between the spin-symmetry axis and the beam-momentum axis at the target, and ϕ is the angle between the spin-symmetry axis and the perpendicular to the reaction plane.⁷ Since the signs of τ_{10} and τ_{20} may be flipped independently at the ion source, a total of three experiments using different spin-symmetry axes (accom-

TABLE I. Summary of experiments performed.

Beam type	Nominal spin orientation		Average measured beam moments ^a			
	β	ϕ	t_{11}	t_{20}	t_{21}	t_{22}
Vector	90°	0°	0.266±0.006	0.014±0.008	-0.009±0.005	0.019±0.008
Tensor	90°	0°	0.004±0.006	0.312±0.008	-0.002±0.006	0.375±0.009
Tensor	0°	90°	-0.002±0.010	0.640±0.008	-0.010±0.011	0.001±0.010
Tensor	54.7°	90°	-0.005±0.003	0.028±0.007	0.300±0.019	-0.229±0.012

^aThe numbers given represent $\frac{1}{2}[t_{kq}^a - t_{kq}^b]$, where the two polarization states a and b result from flipping the sign of the polarization at the ion source. Errors quoted are the variance between a number of measurements.

plished with a spin precessor) was required in order to extract all of the T_{kq} as well as $\sigma_u(\theta)$. These experiments are summarized in Table I.

During all measurements the sign of the beam polarization was flipped by switching rf transitions in the ion source at one second intervals, and the data were stored independently for each beam polarization. Beam intensity modulations between the states of different polarization were measured using a Faraday cup, and were found to be less than 0.1%. All beam moments were measured at regular intervals during the experiment by using a ³He polarimeter⁸ mounted in the beam line downstream from the D₂ gas cell. (To measure the beam polarization the D₂ cell was pivoted out of the beam path.) Thus, the measurements did not depend on the assumption that the deuteron polarization possesses a symmetry axis. The polarization was found to be constant to better than 3% over the course of one week of measurements. The measured values of all beam moments are given in Table I.

In order to extract relative differential cross sections, the number of counts had to be normalized to the product of beam current times target thickness. This was accomplished with a plastic scintillator detector placed at 0° which monitored neutrons from the ²H(d,n)³He reaction. The beam current on target was varied from 150–350 nA in order to keep the singles rate in the NaI detector approximately constant at 200 kHz. In order to perform corrections for deadtime ($\approx 15\%$), a pulser signal, shaped like the NaI detector pulses and with a frequency proportional to the beam current, was introduced into the detector electronics. The cosmic-ray rejection efficiency of the anticoincidence system was measured to be 98%.

III. DATA REDUCTION

Anticoincidence spectra from the NaI detector are shown for three angles in Fig. 1. These spectra are the sum of all measurements and beam polarizations, and represent ~ 24 h of data taking at each angle. The large Q value of the reaction (+ 23.85 MeV) produces a high-energy peak which is separated from a pileup of lower-energy background events. The background is clearly worse at very forward angles, where the detector shielding of events in the upstream beam line is less effective and the ²H(d,n)³He cross section is higher. The separation between the ²H(d, γ) events and the low-energy background improves steadily with increasing lab angle. The smooth curves in the figure represent fits to the measured spectra

with the known line shape of the spectrometer. This line shape was determined from extensive fitting of high-resolution capture γ -ray spectra taken with the same detector. The arrows indicate the peak integration region, which was consistently taken from -8% to +5% of the full energy of the peak. As can be seen, even in the worst case ($\theta_{\text{lab}}=25^\circ$) the low-energy background in the peak integration region is negligible. The yields under the peaks were found by summing all counts in the indicated region and subtracting a constant background (due to unrejected cosmic rays) determined by examining the region above the main peak. Deadtime corrections were applied indi-

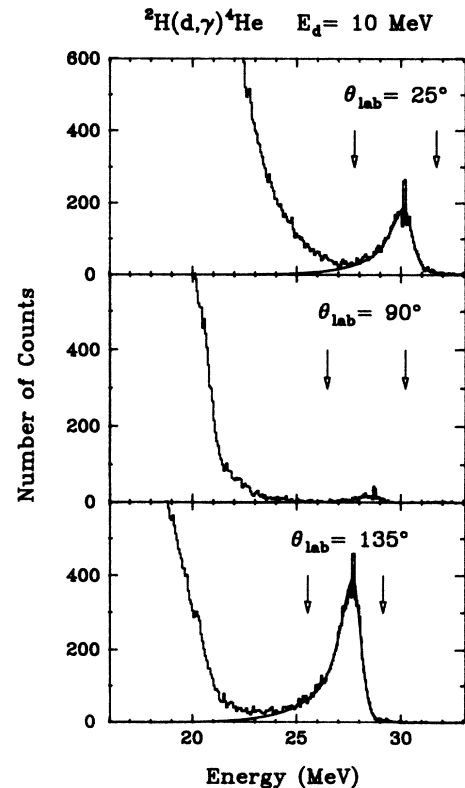


FIG. 1. Anticoincidence γ -ray spectra from the NaI spectrometer at lab angles of 25°, 90°, and 135°. Arrows indicate the peak integration region. The smooth curves are fits of the known γ line shape of the spectrometer to the data.

vidually to the spectra from each polarization state as well as to the neutron monitor spectra.

The data have been corrected for finite geometry of both the target and the detector. The results of the differential cross section measurements, normalized to the absolute cross section measurements of Ref. 9, are shown in Fig. 2. Error bars shown reflect the variance between a dozen or more independent measurements at each angle. The results of the analyzing power measurements are shown in Fig. 3. The error bars reflect primarily counting statistics but also include uncertainties in the background subtraction and beam polarization. Earlier, somewhat less accurate results for $T_{20}(\theta)$ at 9.7 MeV (Ref. 1) are in good agreement with the present data.

IV. ANALYSIS

A. Angular distribution expansions

The expressions for the angular distribution of γ rays from capture reactions have been presented in detail by Seyler and Weller.¹⁰ For clarity we will reproduce Eqs. (7) and (11) of their paper which represent the expansion of the measured cross sections in terms of associated Legendre polynomials:

$$\begin{aligned} \sigma_u(\theta) &= \left(\frac{1}{2}\lambda\right)^2 \hat{x}^{-2} \hat{a}^{-2} \sum_k a_k P_k(\cos\theta) \\ &= A_0 \left[1 + \sum_{k=1} \bar{a}_k P_k(\cos\theta) \right], \end{aligned} \quad (3)$$

$$\begin{aligned} \sigma(\theta) &= \left(\frac{1}{2}\lambda\right)^2 \hat{x}^{-2} \hat{a}^{-2} \sum_k [a_k P_k(\cos\theta) + b_k P_k^1(\cos\theta) p_y \\ &\quad + c_k P_k(\cos\theta) t_{20} \\ &\quad + d_k P_k^1(\cos\theta) \text{Re}(t_{21}) \\ &\quad + e_k P_k^2(\cos\theta) \text{Re}(t_{22})]. \end{aligned} \quad (4)$$

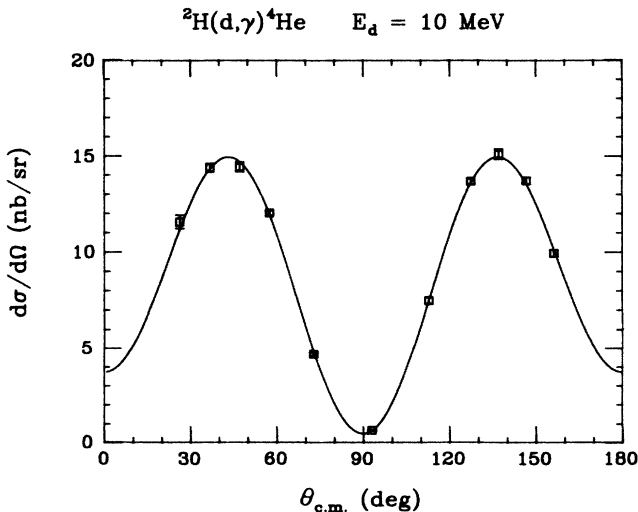


FIG. 2. Differential cross sections measured in the present work and normalized to the results of Ref. 9. The solid line is a Legendre polynomial fit to the data.

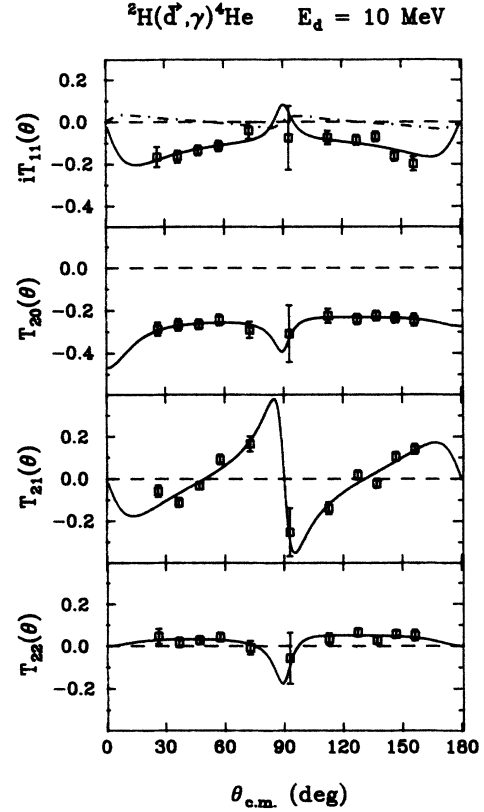


FIG. 3. Vector and tensor analyzing powers measured in the present work. The solid lines are the results of associated Legendre polynomial fits described by Eqs. (5)–(8). The dot-dashed line is a calculation of the vector analyzing power assuming pure $E2$ radiation.

Here λ is the reduced wavelength of the incident beam, x the spin of the projectile, a the spin of the target, the notation $\hat{x} = (2x + 1)^{1/2}$, $\hat{a} = (2a + 1)^{1/2}$, $\bar{a}_k = a_k/a_0$, and $A_0 = \sigma_t/4\pi$. By comparing Eqs. (1), (3), and (4), and recalling that $p_y = 2/\sqrt{3}\text{Re}(it_{11})$, we obtain four equations for associated Legendre polynomial expansions of the products of the unpolarized cross section with the analyzing powers:

$$\sigma_u(\theta) iT_{11}(\theta) = \frac{A_0}{\sqrt{3}} \sum_k \bar{b}_k P_k^1(\cos\theta), \quad (5)$$

$$\sigma_u(\theta) T_{20}(\theta) = A_0 \sum_k \bar{c}_k P_k(\cos\theta), \quad (6)$$

$$\sigma_u(\theta) T_{21}(\theta) = \frac{A_0}{2} \sum_k \bar{d}_k P_k^1(\cos\theta), \quad (7)$$

$$\sigma_u(\theta) T_{22}(\theta) = \frac{A_0}{2} \sum_k \bar{e}_k P_k^2(\cos\theta), \quad (8)$$

where $\bar{b}_k = b_k/a_0$, etc. The solid curves in Figs. 2 and 3 represent the results of least-squares fits of such expansions (up to order $k=4$) to the data. The least-squares procedure indicated no evidence for additional terms of order $k > 4$. The values of the expansion coefficients and χ^2 values obtained are given in Table II. We do not know the reason for the rather poor fit to $\sigma_u(\theta)T_{21}(\theta)$.

TABLE II. Expansion coefficients for the cross section and the products of the cross section with the analyzing powers.

k	$\sigma_u(\theta)$ \bar{a}_k	$\sigma_u(\theta)iT_{11}(\theta)$ \bar{b}_k	$\sigma_u(\theta)T_{20}(\theta)$ \bar{c}_k	$\sigma_u(\theta)T_{21}(\theta)$ \bar{d}_k	$\sigma_u(\theta)T_{22}(\theta)$ \bar{e}_k
0			-0.253 ± 0.009		
1	a	-0.205 ± 0.018	-0.038 ± 0.018	0.000 ± 0.017	
2	0.836 ± 0.013	-0.018 ± 0.016	-0.225 ± 0.023	-0.003 ± 0.015	0.023 ± 0.006
3	a	-0.142 ± 0.012	-0.005 ± 0.030	-0.002 ± 0.011	-0.006 ± 0.004
4	-1.394 ± 0.012	-0.006 ± 0.012	0.313 ± 0.032	-0.124 ± 0.011	0.012 ± 0.002
χ^2/ν	1.37	1.40	0.11	3.79	0.52

^aDue to the symmetry imposed by the identity of the incident and target particles $a_1 = a_3 = 0$.

B. Partial wave analysis

The associated Legendre expansion coefficients thus determined may, in turn, be expressed in terms of the elements of the transition matrix. The allowed transitions of multipolarity $L \leq 2$ for the ${}^2\text{H}(d,\gamma){}^4\text{He}$ reaction are given in Table III using the channel-spin representation ${}^{2s+1}l_j$. Note that the identity of the incident and target deuterons imposes the symmetry condition that the sum of l and s be even. The eight partial wave amplitudes and seven undetermined phase differences form a set of 15 unknown quantities. These quantities appear in the 19 equations for the known associated Legendre expansion coefficients [see Eqs. (20)–(25) of Ref. 10] and are thus determined. A least-squares procedure was employed to extract the values of the partial wave amplitudes and phases from the expansion coefficients, and the results are given in Table III.

It is interesting to note the effects of selectively excluding transitions of a particular multipolarity from these calculations, because many arguments exist for the suppression of various multipoles in this reaction.^{1,2} The reaction proceeds primarily via ($E2$; 1D_2) capture to the predominant 1S_0 state of ${}^4\text{He}$. Since the spin-dependent part of the $E2$ operator is negligibly small at this energy,¹¹ the remaining $E2$ transitions will be comparatively suppressed because they occur only through processes involving the tensor force. The ($E1$; 3P_1) transition is forbidden in the long-wavelength approximation by conservation of isospin in a self-conjugate nucleus. The ($M1$;

5D_1) transition should also be strongly suppressed between states of equal isospin and, again, can occur only via the tensor force. The $M2$ strength should of course be small compared to $E2$. The results of the least-squares fits to the measured angular distribution coefficients for all possible combinations of other multipoles with $E2$ radiation are given in Table IV. Also given are the various multipole contributions to the total cross section obtained from the relevant amplitudes. As can be seen, the assumption of pure $E2$ radiation (even including capture to the ${}^4\text{He}$ D state) is a poor one. Although the differential cross section and tensor analyzing powers may be reasonably reproduced by assuming pure $E2$ radiation, the presence of either $E1$ or $M2$ radiation is required to reproduce the vector analyzing power. This is shown graphically in Fig. 3, where the dot-dashed curve represents $iT_{11}(\theta)$ calculated from the best-fit transition matrix using the pure $E2$ assumption. It seems clear, based upon the χ^2 results, that at least three multipoles must contribute. The case for $E1$ radiation is strengthened by the fact that its exclusion requires a rather unbelievable 20% $M2$ strength in order to reproduce the data (mainly the large, fore-aft symmetric vector analyzing power). It does seem conclusive, in addition, that some $M2$ radiation is present.

C. Evidence of tensor-force effects

The present results also permit an estimate of the extent to which the tensor force plays a role in this reaction. As mentioned above, the inclusion of the tensor component

TABLE III. Allowed transitions, amplitudes, and phases in ${}^2\text{H}(d,\gamma){}^4\text{He}$.

Initial (two-deuteron) state	γ multipolarity	Amplitude	Phase (deg)	Final (${}^4\text{He}$) state ^a
3P_1	$E1$	0.279 ± 0.092	-171 ± 10	${}^1S_0, {}^5D_0$
5D_1	$M1$	0.134 ± 0.046	115 ± 11	5D_0
1D_2	$E2$	1.209 ± 0.015	0^b	1S_0
5S_2	$E2$	0.392 ± 0.047	126 ± 4	5D_0
5D_2	$E2$	0.255 ± 0.072	-75 ± 7	5D_0
5G_2	$E2$	0.008 ± 0.041	53 ± 219	5D_0
3P_2	$M2$	0.241 ± 0.066	44 ± 12	${}^1S_0, {}^5D_0$
3F_2	$M2$	0.072 ± 0.102	1 ± 57	${}^1S_0, {}^5D_0$

^aNeglects tensor-force effects in the entrance channel (see the text).

^bSince only phase differences enter into the calculations, one phase may be arbitrarily set to zero.

TABLE IV. Results of fitting angular distribution coefficients with selected multipoles.

Allowed multipoles	χ^2/ν	Partial contributions to the total cross section (%)				${}^4\text{He}$ final state ^a	
		$E1$	γ multipolarity		$M2$	1S_0	5D_0
$E2$	38.87			$E2$		85.7±0.08	14.3±1.4
$M1,E2$	27.81		2.2±0.6	$E2$		83.1±3.8	16.9±4.5
$E2,M2$	22.69			$E2$	7.0±0.8	84.8±3.7	15.2±3.7
$E1,E2$	17.29	8.0±0.8		$E2$		86.2±4.1	13.8±4.2
$E1,M1,E2$	5.36	8.7±0.8	2.4±0.6	$E2$		84.1±4.4	15.9±4.5
$M1,E2,M2$	1.54		2.1±0.4	$E2$	19.6±1.2	68.8±9.9	31.2±9.9
$E1,E2,M2$	1.20	6.5±2.4		$E2$	5.2±1.9	79.9±5.6	20.1±5.9
$E1,M1,E2,M2$	0.42	2.6±1.7	0.6±0.4	$E2$	3.5±1.9	84.2±3.2	15.8±3.9

^aNeglects tensor-force effects in the incident channel (see the text).

of the nucleon-nucleon interaction gives rise to the 5D_0 component in the ${}^4\text{He}$ ground state. If, for the moment, we neglect the tensor force in the incident channel, as done in Refs. 1 and 2, then the arguments made in Sec. IV B show that the $M1$ and $E2$ transitions (which account for $\sim 90\%$ of the measured cross section) each have a unique final state (either 1S_0 or 5D_0) in ${}^4\text{He}$ (see Table III). Under this assumption we may calculate the partial contributions to the total cross section from both S -state and D -state capture using the appropriate partial wave amplitudes (while allowing for complete uncertainty with regard to the final state of the $E1$ and $M2$ transitions). The results, given in Table IV, indicate that no matter what assumptions are made regarding allowed multipoles, a large part ($\sim 15\%$) of the capture cross section arises from capture to the D state.

There is, however, no justification for ignoring possible effects of the tensor force in the incident channel. The inclusion of the deuteron (internal) D state or of angular-momentum mixing due to the tensor force between the two deuterons in the incident channel breaks down the unique one-to-one relationship between the initial (two-deuteron) and the final (α -particle) state for the $E2$ transitions. The magnitude of these effects, compared to the tensor-force effect which gives rise to the ${}^4\text{He}$ D state in the exit channel, is difficult to estimate and cannot be determined from the measurements. As pointed out by Weller *et al.*,¹² the mixing of the $J=2$ states for the $E2$ transition may be important at this energy. Certainly the D -state amplitude of the deuteron is comparable to that of ${}^4\text{He}$. It is not possible, therefore, to make any direct conclusion about the D -state admixture in ${}^4\text{He}$. On the other hand, the present results do provide evidence that the tensor force affects this reaction at the level of 15% of the capture cross section.

V. CONCLUSIONS

Because of the symmetry involved, angular distribution measurements of the differential cross section and vector and tensor analyzing powers in the ${}^2\text{H}(\vec{d},\gamma){}^4\text{He}$ reaction completely determine the elements of the transition matrix for multipoles $L \leq 2$ and, therefore, the various multipole strengths.

Because it is not possible in the partial-wave analysis to distinguish between the effect of the tensor force in the exit channel (as manifested by capture to the D state of ${}^4\text{He}$) and tensor-force effects in the incident channel (which eliminate the one-to-one correspondence between the incident partial waves and the final ${}^4\text{He}$ state), it is not possible to make a quantitative statement about the D -state amplitude in ${}^4\text{He}$. We may, however, conclude that the tensor force plays a significant role in this reaction, affecting the cross section at the level of 15%, whether such effects occur in the entrance or exit channel.

While the assumption of pure $E2$ radiation^{1,2,12} is reasonable at the 80–90% level, and while one may apply such an assumption if one merely wishes to generate fits to the differential cross section or tensor analyzing powers, it becomes evident when the vector analyzing power data are included that other multipoles must be present at the 10–20% level. Since the ${}^4\text{He}$ D -state effects one wishes to investigate are at about the same level, it would be unreasonable to ignore other multipoles.

Finally, one must be careful not to equate the ($E2$; 5S_2) transition with ${}^4\text{He}$ D -state effects, as is done in Ref. 12. Quite simply, one deuteron in the S state and another in the D state with relative angular momentum $L=0$ may capture to the 1S_0 component of the ${}^4\text{He}$ ground state in an $E2$ transition involving no spin flip. Furthermore, two deuterons asymptotically in the 5S_2 state may be mixed via the tensor force with another of the $J=2$ states.

It is hoped that the present results will stimulate further work on the theory of the magnitude of these tensor-force effects in the incident channel, for only after this difficult theoretical problem has been solved can the ${}^2\text{H}(\vec{d},\gamma){}^4\text{He}$ reaction be used as a reliable tool for the determination of the ${}^4\text{He}$ D -state amplitude.

ACKNOWLEDGMENTS

We are grateful to Prof. S. Hanna and Prof. F. D. Santos for helpful discussions during the course of this project. This work was supported by the U.S. National Science Foundation under Grant No. PHY-8414810.

*Present address: Physics Department, Gustavus Adolphus College, St. Peter, MN 56082.

¹H. R. Weller, P. Colby, N. Roberson, and D. R. Tilley, *Phys. Rev. Lett.* **53**, 1325 (1984).

²F. D. Santos, A. Arriaga, A. M. Eiro, and J. A. Tostevin, *Phys. Rev. C* **31**, 707 (1985).

³S. Mellema, T. R. Wang, and W. Haerberli, *Phys. Lett.* **166B**, 282 (1986).

⁴W. Haerberli *et al.*, *Nucl. Instrum. Methods* **196**, 319 (1982).

⁵C. A. Gossett, Ph.D. thesis, University of Wisconsin, 1983.

⁶E. M. Diener, J. F. Amann, S. L. Blatt, and P. Paul, *Nucl. Instrum. Methods* **83**, 115 (1970).

⁷W. Haerberli, in *Nuclear Spectroscopy and Reactions, Part A*, edited by J. Cerny (Academic, New York, 1975), p. 15.

⁸K. Stephenson and W. Haerberli, *Nucl. Instrum. Methods* **169**, 483 (1980).

⁹W. E. Meyerhof, W. Feldman, S. Gilbert, and W. O'Connell, *Nucl. Phys.* **A131**, 489 (1969).

¹⁰R. G. Seyler and H. R. Weller, *Phys. Rev. C* **20**, 453 (1979).

¹¹J. M. Eisenberg and W. Greiner, *Excitation Mechanisms of the Nucleus* (North-Holland, Amsterdam, 1970), Vol. 2, p. 109.

¹²H. R. Weller *et al.*, *Phys. Rev. C* **34**, 32 (1986).